

Modeling of quantal neurotransmitter release kinetics in the presence of fixed and mobile calcium buffers

Iskander R. Gilmanov · Dmitry V. Samigullin ·
František Vyskočil · Eugeny E. Nikolsky ·
Ellya A. Bukharaeva

Received: 12 August 2007 / Revised: 21 December 2007 / Accepted: 17 January 2008 / Published online: 22 April 2008
© Springer Science + Business Media, LLC 2008

Abstract The local calcium concentration in the active zone of secretion determines the number and kinetics of neurotransmitter quanta released after the arrival of a nerve action potential in chemical synapses. The small size of mammalian neuromuscular junctions does not allow direct measurement of the correlation between calcium influx, the state of endogenous calcium buffers determining the local concentration of calcium and the time course of quanta exocytosis. In this work, we used computer modeling of quanta release kinetics with various levels of calcium influx and in the presence of endogenous calcium buffers with

varying mobilities. The results of this modeling revealed the desynchronization of quanta release under low calcium influx in the presence of an endogenous fixed calcium buffer, with a diffusion coefficient much smaller than that of free Ca^{2+} , and synchronization occurred upon adding a mobile buffer. This corresponds to changes in secretion time course parameters found experimentally (Samigullin et al., *Physiol Res* 54:129–132, 2005; Bukharaeva et al., *J Neurochem* 100:939–949, 2007).

Keywords Neuromuscular junction · Mathematical modeling · Time course of secretion · Calcium buffers

Action Editor: Upinder Bhalla

I. R. Gilmanov · D. V. Samigullin · E. E. Nikolsky ·
E. A. Bukharaeva
Institute of Biochemistry and Biophysics,
Russian Academy of Sciences,
P.O. Box 30, Kazan 420111, Russia

E. A. Bukharaeva
e-mail: ellyab@mail.ru

F. Vyskočil
Department of Animal Physiology and Developmental Biology,
Faculty of Sciences, Charles University,
Viničná 7,
Prague 2, Czech Republic

F. Vyskočil (✉)
Institute of Physiology,
Academy of Sciences of the Czech Republic,
Videňská 1083,
142 20 Prague 4, Czech Republic
e-mail: vyskocil@biomed.cas.cz

E. E. Nikolsky · E. A. Bukharaeva
Kazan State Medical University,
Butlerov st. 49,
Kazan 420012, Russia

Abbreviations

TCS time course of secretion
BAPTA-AM 1,2-bis(2-aminophenoxy)ethane-*N,N,N,N*-
tetraacetic acid tetrakis acetoxymethyl ester

1 Introduction

The release of neurotransmitters from presynaptic nerve endings in response to a nerve impulse takes place in the region of active secretion zones as a result of the entry of calcium ions (Ca^{2+}) through voltage-gated calcium channels, which are opened during the depolarization of the nerve ending by an action potential (Katz 1968; Augustine 2001). The release probability of the neurotransmitter quanta in response to the nerve impulse, which determines its quantity (quantal content), depends on the concentration of Ca^{2+} in the active zone (Augustine 2001; Katz and Miledi 1965). Changes in the probability of quantal secretion with time, i.e., the kinetics of the process, are determined (a) by the local concentration of Ca^{2+} in the

region of release, which in turn depends on the amount of entering calcium, (b) by the distance between the site of Ca^{2+} entry and the calcium release sensors, and (c) by the properties of endogenous buffering systems of Ca^{2+} that participate in the rapid decrease in the local concentration of Ca^{2+} in the active zone (Schneggenburger and Neher 2005; Burnashev and Rozov 2005). Using flash photolysis and uncaging techniques, making it possible to control the intracellular content of Ca^{2+} , direct experimental evidence of calcium regulation of the release kinetics of the neurotransmitter was found in the synaptic contacts of the central nervous system (pyramidal neurons, Held's calyx cells; Lin and Farber 2002; Schneggenburger and Neher 2005). Nevertheless, the abilities of present-day methods to visualize Ca^{2+} in the tiny packed presynaptic buttons of the rat and mouse endplate do not permit the direct determination of the relationship between the time course of calcium transients and timing of quanta release. One of the ways of quantitatively describing these rapid processes, determining the kinetics of Ca^{2+} concentration changes near the secretion area and their relationship to the kinetics of evoked quanta release, is mathematical modeling (Yamada and Zucker 1992; Klingauf and Neher 1997; Matveev et al. 2002, 2004).

In our recent experiments with the mouse neuromuscular synapse, we showed that Ca^{2+} ions modify the time course of release of acetylcholine (Samigullin et al. 2005; Bukharaeva et al. 2007). The decrease in extracellular Ca^{2+} lowered the quantal content as expected and caused an increase in the fluctuations of synaptic delays; that is, it desynchronized secretion. In contrast, a change in the intracellular Ca^{2+} content with the aid of the mobile calcium buffer 1,2-bis(2-aminophenoxy)ethane-*N,N,N,N*-tetraacetic acid tetrakis acetoxymethyl ester (BAPTA-AM; exhibiting rapid binding kinetics) caused a decrease in the fluctuation of synaptic delays, i.e., an increase in secretion synchrony. Despite the fact that, in both cases, a decrease in the number of quanta was found to be due to a decrease in intracellular calcium, the secretion kinetics changed in opposite directions. To clarify how the intracellular processes that locally distribute Ca^{2+} are involved in quanta release, we set out to model the time course of secretion (TCS) of the neurotransmitter in the active secretion zone during changes in Ca^{2+} concentration and in the presence of calcium buffering systems of varying mobilities. The importance of assessing the role of calcium buffers is supported by the fact that only 1–5% of the entering Ca^{2+} can be considered to be “free” calcium (Ahmed and Connor 1988), whereas the vast majority of the entering calcium is practically immediately bound to calcium-binding sites, the mobility of which determines the nature of Ca^{2+} diffusion from their entry region into nerve endings and the sites where vesicles are docked (Zhou and Neher 1993; Gabso et al.

1997; Muller et al. 2005). The model—in agreement with previous experiments (Samigullin et al. 2005; Bukharaeva et al. 2007)—showed that the presence of an endogenous fixed calcium buffer, the diffusion coefficient of which is very much smaller than the diffusion coefficient of free Ca^{2+} , brings about the desynchronization of secretion under conditions of decreased extracellular Ca^{2+} and synchronization upon adding a mobile buffer.

2 Methods

2.1 Model description

The model of the active zone is represented as an assembly of a point source of calcium ion entry (the voltage-gated calcium channel), synaptic vesicles (calcium sensors), located at a distance 50 nm from the point of calcium entry, and of a fixed or mobile calcium buffer (for the general scheme, see Fig. 1).

In the modeling process, it was assumed that Ca^{2+} moves from the extracellular medium into the region of the active secretion zone and passes through a singular source of sufficiently small cross-section, which can be considered point like. No active transport of Ca^{2+} across the membrane is postulated, as according to the data of Lin et al. (2005)—blocking Ca^{2+} extrusion or Ca^{2+} sequestration processes did not significantly alter the kinetics of Ca^{2+} concentration changes, arguing against a role for either mechanism. This made it possible to consider the diffusion process in the active zone to be a homogeneous diffusion due to the spherical symmetry of the region.

The presence of vesicles near the plasma membrane can change the spatial profiles of Ca^{2+} concentration because

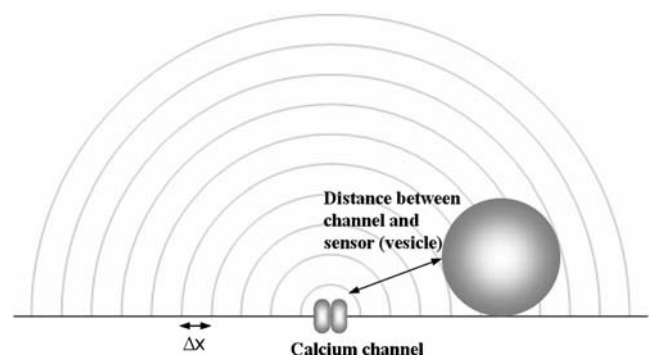


Fig. 1 Scheme of the modeled active zone. Calcium channel—a point source of calcium ion entry. Synaptic vesicle (calcium sensor) is located 50 nm from the point of calcium entry. The volume within which the diffusion was modeled was divided into concentric hemispherical layers of different radii, the difference between neighboring layers being Δx . The distance between layers Δx was set to 2 nm

the vesicles acts as a diffusion barrier after the Ca^{2+} channel is opened. But in this work, we did not take the role of vesicles as a diffusion barrier into account, as using the Monte Carlo simulation, Glavinovich and Rabie (2001) showed that the presence of a vesicle of diameter 50 nm at a distance of 50 nm from the calcium entry point did not significantly alter the distribution of calcium concentration near the calcium sensor (see Fig. 1 in the paper Glavinovich and Rabie 2001).

We only consider one calcium channel in the model to simplify the calculation. Such an assumption is permissible, as it was shown by Shahrezaei et al. (2006) that the response to the action potential in the neuro-muscular synapse leads to the opening of one or two calcium channels within a single active secretion zone.

The volume in which the diffusion was modeled was divided into concentric hemispherical layers of increasing radii, the difference between neighboring layers was Δx , and the entry rate of calcium was considered to be the corresponding increase in Ca^{2+} concentration in the central volume (hemisphere of radius Δx) within the time Δt (Fig. 1). The size of Δt was taken to be 0.005 μs , the distance between layers Δx was 2 nm. The radius of the modeled volume was 600 nm.

The Ca^{2+} flux was modeled as a constant inward current more than 0.5 ms (the kinetics of channel opening and the residual fluxtail current were not considered). The different extracellular concentrations of Ca^{2+} ions were modeled as currents of differing magnitudes (0.3 and 0.9 pA) but of the same duration. Diffusive changes in the concentration of Ca^{2+} , buffers, and Ca^{2+} -buffer complexes in the various volumes were calculated by the following equation

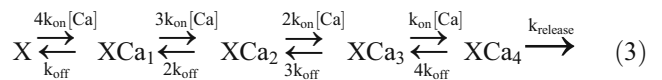
$$\Delta C_i = (D\Delta t/V_i\Delta x)[S_{i-1}(C_{i-1} - C_i) - S_i(C_i - C_{i+1})] \quad (1)$$

where C_i is the concentration of the corresponding molecules in the i -th volume, D the diffusion coefficient for the given type of molecule, S_i is the surface area through which diffusion takes place, Δx is the difference in radii of neighboring layers, and Δt is the selected time step. The formation of complexes of Ca^{2+} with the buffers was modeled by the following:

$$\Delta[\text{Ca}]_i = \Delta[\text{B}]_i = -\Delta[\text{CaB}]_i = (k_{\text{off}}[\text{CaB}]_i - k_{\text{on}}[\text{Ca}]_i[\text{B}]_i)\Delta t \quad (2)$$

where $\Delta[\text{Ca}]_i$ is the change in Ca^{2+} concentration in the i -th volume over the time Δt , $\Delta[\text{B}]_i$ is the change in concentration of the corresponding buffer, $\Delta[\text{CaB}]_i$ is the change in concentration of the corresponding complex of Ca^{2+} with the buffer, and k_{on} and k_{off} are rate constants.

The binding of Ca^{2+} with the sensor and the rate of release were calculated according to the scheme:



where X refers to the secretion sensor and XCa to the sensor bound with Ca^{2+} ions. The distance at which the Ca sensor was located from the ion entry point, i.e., from the calcium channel, was taken as 50 nm. The number of Ca-binding sites on the sensor was taken to be four, on the basis of the coefficient of cooperativity for Ca^{2+} (Dodge and Rahamimoff 1967).

The TCS is the envelope curve of the frequency histogram of the delays of quanta release (Fig. 2) or, as a cumulative curve, which is a function of cumulative frequencies (integral of TCS), reveals the temporal distribution of the quanta releases that form the end plate current after the arrival of the nerve impulse (Katz and Miledi 1965; Van der Kloot 1988).

In our model, the value of the TCS at time t is the number of quanta released in the time interval Δt according to the equation:

$$\text{TCS}(t) = k_{\text{rel}}[\text{XCa}_4](t)\Delta t \quad (4)$$

where the values of X and XCa $_i$ were normalized to X_0 (value X at time $t=0$ when $[\text{XCa}_i]=0$), so the TCS was obtained as the activated proportion of the initial number of calcium sensors X_0 .

The numerical values of the parameters used in the model are shown in the Table 1 and are based on literature references.

Simulations were performed with custom-written codes using Free Pascal Compiler (www.freepascal.org). Our

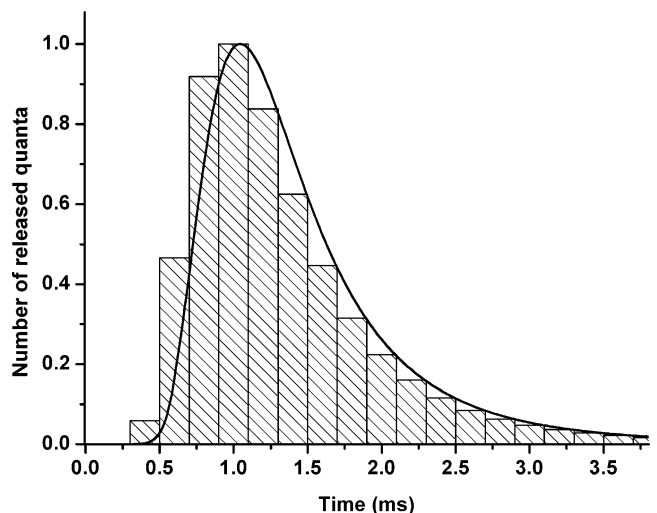


Fig. 2 The histogram of the quantal release times and the curve of the TCS obtained from the model

Table 1 The numerical values of constants for model parameters

Parameter	Value	References
Δt for diffusion model	0.005 μs	— ^a
Δx	2 nm	—
Initiation of calcium current	0.1 ms	—
Duration of calcium current	0.5 ms	—
Number of Ca sites on receptor	4	—
k_{on} Ca to receptor	0.1 $\mu\text{M}^{-1} \text{ms}^{-1}$	—
k_{off} Ca from receptor	5 ms^{-1}	Schneggenburger and Neher 2000
k_{release}	5 ms^{-1}	Bennett et al. 2000; Shahrezaei and Delaney 2004
Radius of simulation volume	600 nm	—
Ca sensor distance from channel	50 nm	—
Calcium diffusion	223 $\mu\text{m}^2 \text{s}^{-1}$	Tang et al. 2000
Endogenous fixed buffer concentration	8000 μM	Matveev et al. 2002
Endogenous fixed buffer diffusion	0	—
Endogenous fixed buffer k_{on}	0.5 $\mu\text{M}^{-1} \text{ms}^{-1}$	Kits et al. 1999; Matveev et al. 2002
Endogenous fixed buffer k_{off}	8 ms^{-1}	Matveev et al. 2002
BAPTA concentration	500 μM	Kits et al. 1999; Segura et al. 2000
BAPTA diffusion	220 $\mu\text{m}^2 \text{s}^{-1}$	Meinrenken et al. 2002
BAPTA k_{on}	0.4 $\mu\text{M}^{-1} \text{ms}^{-1}$	Segura et al. 2000; Meinrenken et al. 2002
BAPTA k_{off}	0.088 ms^{-1}	Segura et al. 2000; Meinrenken et al. 2002

^a Obtained by the modeling parameters.

source codes are available at <http://timecourse.nm.ru>. Integration was performed using a simple rectangle method, which due to the small Δt and Δx , did not introduce a large error.

We have verified the accuracy of our calculations, having compared them to the results of analytical calculations of the diffusion of calcium. Besides this, calculations of the diffusion of calcium have been carried out using the Calcium Calculator by Matveev (<http://web.njit.edu/~matveev/calc.html>). The results obtained were similar to our model.

3 Results

3.1 Changes in calcium concentration and TCS dependence on the size of calcium flux in the absence of calcium buffers

Figure 3(a) and (b) shows changes in Ca^{2+} concentration (absolute and normalized to the amplitude) at a distance of 50 nm from the calcium entry point at two different calcium fluxes through the channel. Due to the high rate of diffusion of Ca^{2+} , in the absence of any buffer within a distance of several tens of nanometers from the channel, the intracellular concentration of Ca^{2+} rapidly reaches a near-equilibrium level. Curves of calcium concentration changes at the sensor, corresponding to different calcium fluxes, differ in amplitude but are identical in form.

Although the kinetics of Ca^{2+} concentration changes at the sensor at different channel fluxes, which differs only in amplitude, the shape of the TCS is different for Ca^{2+} fluxes corresponding to 0.3 and 0.9 pA [Fig. 3(c)]. With the stronger flux, the TCS rises more rapidly due to an increased number of quanta secreted with a smaller synaptic delay. In other words, the early phase of quanta release is accelerated. The phases of TCS decrease corresponding to the late phase of secretion are identical, in as much as they are defined by the rate of exocytosis and dissociation of Ca^{2+} from the sensor, rather than by the rate of dissipation of calcium concentration in the vicinity of the sensor.

In this way, the increased amplitude of Ca^{2+} flux by approximately a factor of 3 is not accompanied by changes in the kinetics of Ca^{2+} concentration, but it introduces small changes in the character of secretion. The probability of secretion with short delays increases, but the probability of secretion with longer delays remains the same.

3.2 Changes in calcium concentration and TCS dependence on the value of Ca^{2+} flux in the presence of a mobile buffer

The presence of a mobile Ca^{2+} buffer with a diffusion coefficient equal to the diffusion coefficient of free Ca^{2+} , at an identical rate of Ca^{2+} flux, produces changes in the parameters of Ca^{2+} concentration kinetics.

Figure 4(a) and (b), respectively, shows the changes in Ca^{2+} concentration (absolute and normalized to the amplitude) at the sensor with and without a mobile buffer.

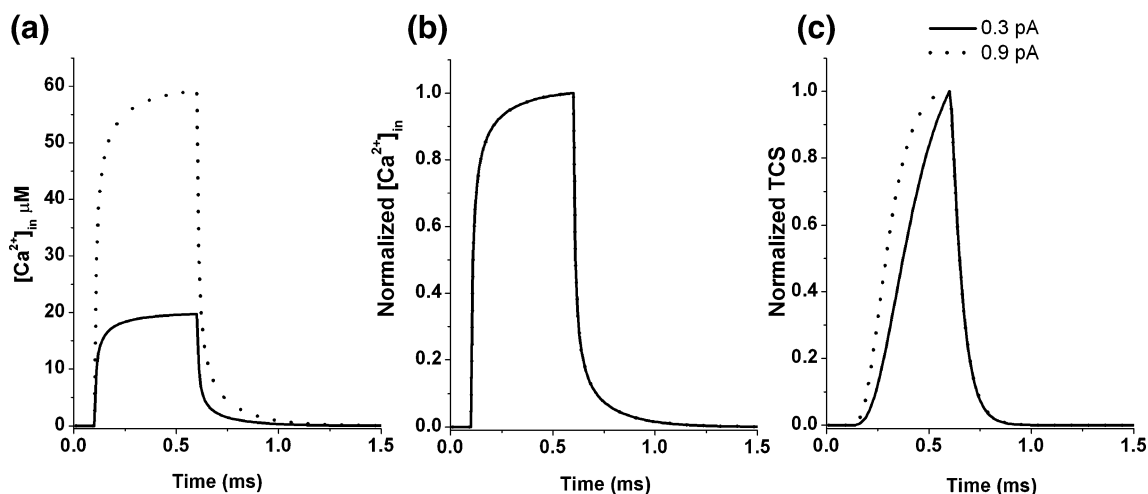


Fig. 3 (a) Changes in Ca^{2+} concentration at different channel flux intensities (0.3 and 0.9 pA). (b) Normalized graphs of Ca^{2+} changes at flux intensities of 0.3 and 0.9 pA (they are identical). (c) TCS at flux intensities through the channel equal to 0.3 and 0.9 pA

Besides the decreased absolute value of the calcium concentration maximum [Fig. 4(a)], the presence of a mobile buffer brings about a more rapid attainment of the concentration maximum and acceleration of its fall [Fig. 4(b)]. The TCS curves, however, are practically identical for the situation with and without buffer.

Figure 5(a),(b), and (c) shows the curves of changes in Ca^{2+} concentration (absolute and normalized to the amplitude) and the TCS in the presence of a mobile buffer at two different flux intensities. The presence of a mobile buffer removes the differences in the rise time of the TCS observed at two calcium fluxes without buffer [Fig. 3(c)]. As the mobile buffer makes the decay in calcium concentration faster, the fall in the TCS, as before, is defined by the rates of exocytosis and dissociation of Ca^{2+} from the sensor and does not change at different intensities of channel flux [Fig. 5(c)]. In this way, the presence of the

mobile calcium buffer alone, due to rapid diffusion, removes the changes in the early secretion phase, observed at different values of calcium flux without buffers, and the late secretion phase remains insensitive to both the presence of the buffer and the magnitude of calcium flux.

3.3 Changes in calcium concentration and TCS secretion dependence on the size of calcium flux in the presence of a fixed buffer

Figure 6(a) and (b) shows the changes in Ca^{2+} concentration (absolute and normalized to the amplitude) during changes in flux intensity in the presence of a fixed calcium buffer, i.e., a buffer with molecules that change their position very little during the time of secretion, compared with the distance between the channel and the sensor. In the model, the diffusion coefficient for this buffer is equal to

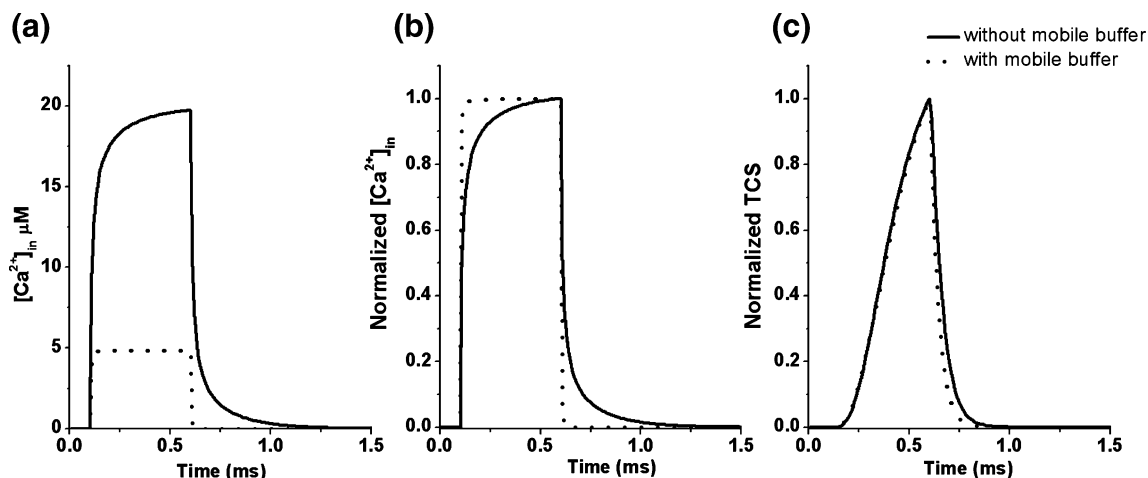


Fig. 4 (a) Changes in Ca^{2+} concentration at channel flux intensity of 0.3 pA in the absence and presence of a mobile Ca^{2+} buffer inside the nerve terminal. (b) Normalized graph of Ca^{2+} concentration changes at a flux intensity of 0.3 pA in the absence and presence of a mobile

Ca^{2+} buffer within the nerve terminal. (c) TCS at a flux intensity across the channel of 0.3 pA in the absence and presence of a mobile Ca^{2+} buffer

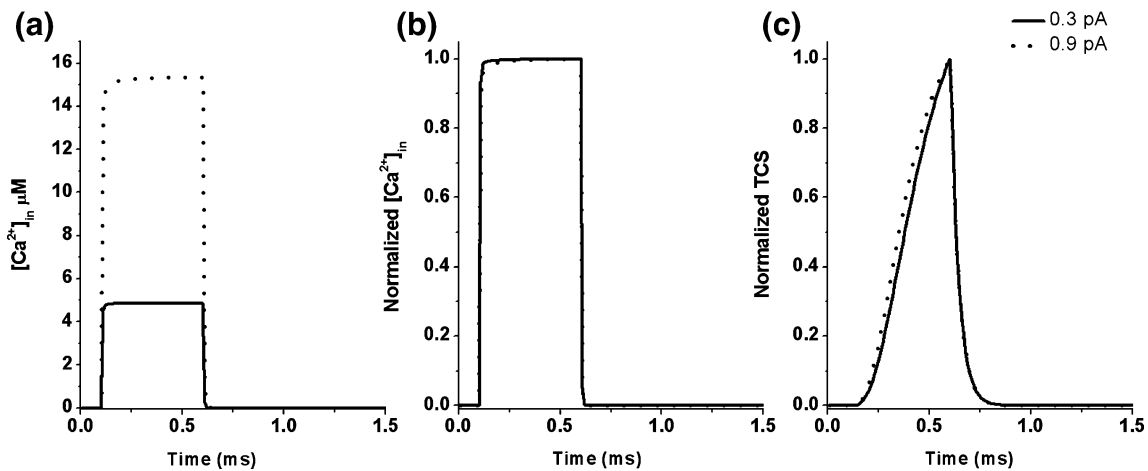


Fig. 5 (a) Ca^{2+} concentration changes in the presence of a mobile buffer with flux intensities through the channel of 0.3 and 0.9 pA. (b) Normalized graphs of calcium concentration changes in the presence

of a mobile Ca^{2+} buffer at flux intensities through the channel of 0.3 and 0.9 pA. (c) TCS in the presence of a mobile Ca^{2+} buffer within the nerve terminal at flux intensities of 0.3 and 0.9 pA

zero, that is, it is assumed that the buffer molecules are completely immobile.

In contrast with the cases described above (without buffer and with a mobile buffer), the kinetics of calcium concentration near the sensor are very different at various magnitudes of flux through the channel, particularly during the phase of Ca^{2+} concentration decay. The decay in Ca^{2+} concentration at low values of calcium flux becomes substantially slower than at higher ones [Fig. 6(a) and (b)].

Moreover, Ca^{2+} concentration at the sensor keeps increasing after the calcium flux through the channel ends (the channel flux begins after 0.1 ms and stops after 0.6 ms).

It is known that the Ca^{2+} concentration peak is delayed relative to the calcium entry rate due to diffusion (Stockbridge and Moore 1984). Equally substantial changes are displayed by the TCS curves for two different calcium fluxes

[Fig. 6(c)]. We observe that, at a low value of calcium flux, the increase and decrease phases of the TCS are longer. Such changes in the kinetics of calcium concentration and in the TCS can be explained by assuming that the fixed buffer delays Ca^{2+} diffusion.

The change in calcium concentration near the sensor is due to Ca^{2+} diffusion from the layers nearest to the channel, diffusion into outer layers and calcium exchange (binding and unbinding) with the fixed buffer. This may be described as:

$$\Delta[Ca]_i = \Delta[Ca]_{in} - \Delta[Ca]_{out} - k_{on}[Ca]_i[B]_i + k_{off}[CaB]_i \quad (5)$$

Therefore, it is possible that a situation could arise after the calcium current has ended in which the calcium inflow from internal layers and release from the buffer will be

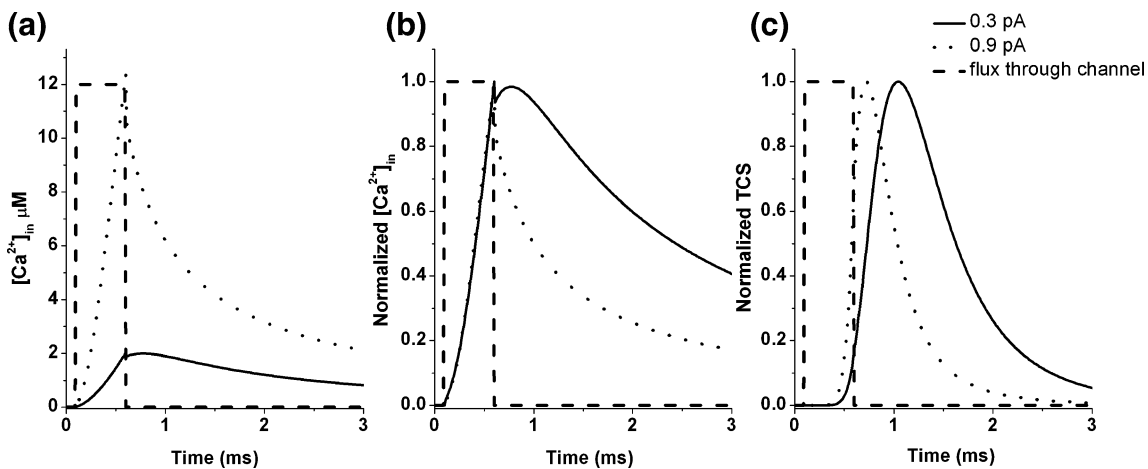


Fig. 6 (a) Change in Ca^{2+} concentration in the presence of a fixed Ca^{2+} buffer within the nerve terminal at flux values of 0.3 and 0.9 pA. Flux through the channel was also recorded. (b) Normalized graphs of calcium concentration changes in the presence of a fixed calcium

buffer within the nerve terminal at channel flux values of 0.3 and 0.9 pA. (c) TCS in the presence of a fixed calcium buffer within the nerve terminal at channel flux values of 0.3 and 0.9 pA

greater than the calcium removal due to diffusion and binding to the buffer:

$$\Delta[\text{Ca}]_{\text{in}} + k_{\text{off}}[\text{CaB}]_i > \Delta[\text{Ca}]_{\text{out}} + k_{\text{on}}[\text{Ca}]_i[\text{B}]_i. \quad (6)$$

In this case, the change in calcium concentration in layer $\Delta[\text{Ca}]_i$ will be positive. In other words, the calcium concentration near the sensor can rise for some time even after the calcium current through the channel has stopped. The slowing down of the decay in Ca^{2+} concentration under low calcium entry in the presence of a fixed buffer leads to the more prolonged decay of the TCS and therefore to an increase in the release asynchrony, as was observed in the experiment (cf. Fig. 8).

3.4 Changes in calcium concentration and TCS in the presence of mobile and fixed buffers

Figure 7(a) and (b) shows calcium concentration changes at the sensor (absolute and normalized to the amplitude) in the presence of a fixed buffer with and without a mobile buffer at an equal value of calcium flux. The presence of the mobile buffer in this case brings about an acceleration of the decay in calcium concentration with little impact on the time to reach its maximum value. The TCS curve in the presence of a mobile buffer exhibits an insignificant acceleration of the increase phase and a substantial shortening of the decrease phase [Fig. 7(c)]. If, in the absence of a fixed buffer, the decay of the TCS curve is defined by the rates of exocytosis and dissociation of Ca^{2+} from the sensor, then upon adding a mobile buffer, the decay begins to be governed by a slow dissipation of calcium from the fixed buffer.

The mobile buffer brings about an acceleration of calcium distribution in the region, which causes a more

rapid termination of the secretion process and, consequently, an acceleration of the decay phase of the TCS curve.

4 Discussion

The purpose of this study was to analyze the kinetics of Ca^{2+} concentration in the area of active secretion with varying Ca^{2+} flux through voltage-gated channels and to evaluate the contribution of endogenous mobile and fixed Ca^{2+} buffers to the determination of the time course of quanta release.

Endogenous Ca^{2+} buffers play a principal role in evoked quantal release (Sala and Hernandez-Cruz 1990; Nowycky and Pinter 1993; Lin et al. 2005). As already stated, after the arrival of the action potential and entry of Ca^{2+} through the voltage-gated channels, more than 95% of the Ca^{2+} ions are immediately bound to the buffers within a distance of 10–50 nm from the point of Ca^{2+} entry (Augustine and Neher 1992a; Neher 1995). Further diffusion of Ca^{2+} is mainly determined by the degree of mobility of the Ca^{2+} -binding components. Fixed binding components, the diffusion rate of which is much lower than the diffusion rate of free Ca^{2+} , can be located on cell organelles or cytoskeleton components. Fixed buffers slow down calcium ion diffusion, prolonging the state of increased Ca^{2+} content in the secretion region (Chow et al. 1994). Numerous intracellular calcium-binding systems (mitochondria, endoplasmic reticulum, Ca-ATPases) can act as calcium chelators that alter the intracellular content of free Ca^{2+} (Zhou and Neher 1993; Schneggenburger and Neher 2000). Mobile calcium buffers, such as soluble Ca^{2+} -binding proteins or small molecules taking part in metabolism (adenosine triphosphate or guanosine triphosphate), have

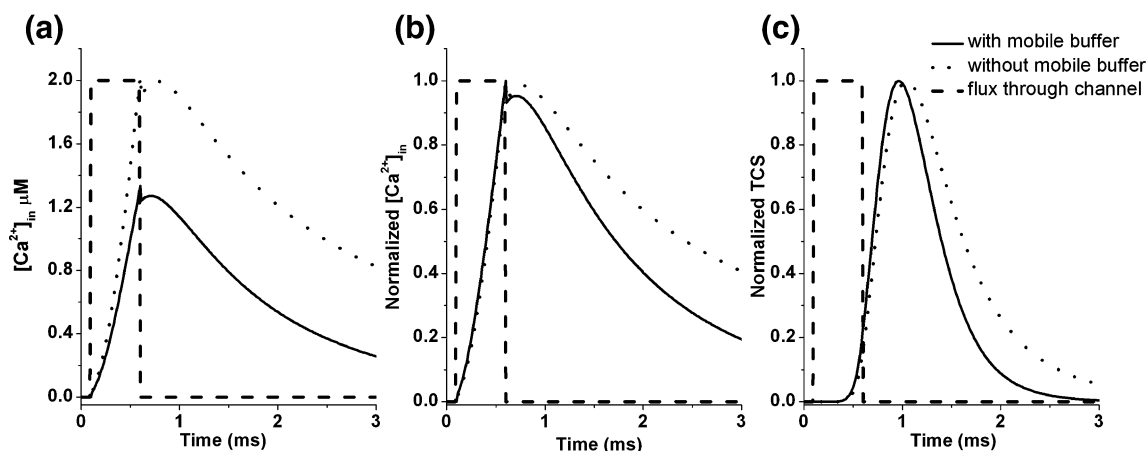


Fig. 7 (a) Changes in Ca^{2+} concentration in the presence of a fixed Ca^{2+} buffer within the nerve terminal (flux intensity across the channel 0.3 pA) with and without a mobile buffer. (b) Normalized graphs of Ca^{2+} concentration changes in the presence of a fixed buffer within the

nerve terminal (flux intensity 0.3 pA) with and without a mobile buffer. (c) TCS in the presence of a fixed calcium buffer within the nerve terminal (flux intensity through the channel 0.3 pA) with and without a mobile buffer

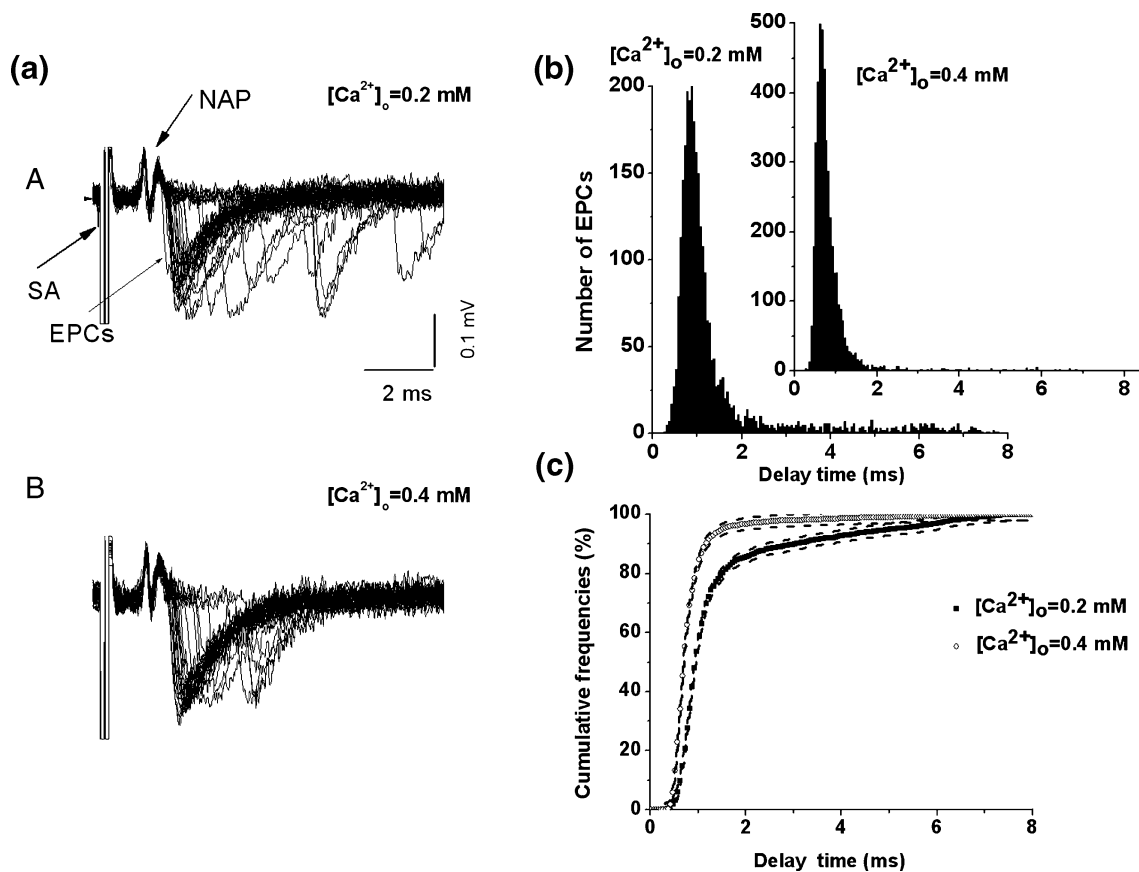


Fig. 8 Experimental data obtained at a single neuromuscular junction at extracellular calcium concentration $[Ca^{2+}]_o = 0.2$ and 0.4 mM . **(a)** Recordings *A* and *B* are superimposed traces of extracellularly recorded presynaptic unquantal endplate currents (*EPCs*) preceded by nerve action potentials (*NAP*). *SA* stimulus artifacts. The time intervals between the peak of the inward presynaptic Na^+ currents of the nerve spike (downward deflection of *NAP*) and the time at which the rising phases of each *EPC* reached 20% of maximum was defined as the release synaptic delay. The traces with failures are not shown; their number was $1,130 \pm 151$ of $1,581 \pm 203$ stimulations for 0.4 mM

Ca^{2+} and $1,804 \pm 267$ of $1,984 \pm 351$ for $0.2 \text{ mM } Ca^{2+}$, respectively. **(b)** Total histograms of synaptic delay values of unquantal *EPCs* [data from four experiments as shown in **(a)**]. Note the presence [with $0.2 \text{ mM } Ca^{2+}$] and absence [with $0.4 \text{ mM } Ca^{2+}$] of long-latency *EPCs*. The bin size was 0.05 ms . **(c)** Cumulative plot from histograms of synaptic delay values. The dotted lines parallel to the curves are confidence limits at $p=0.05$. According to the Kolmogorov–Smirnov criteria, the difference between the curves is statistically significant if the confidence limits of the two curves do not overlap

diffusion coefficients similar to free Ca^{2+} . By dispersing the increased calcium concentration, they bring about increased diffusion and enlarge the zone of Ca^{2+} activity (Augustine and Neher 1992b; Zhou and Neher 1993). Possible candidates for highly mobile calcium buffers are organic ions and such metabolites as maleate, nucleotides, and phosphocreatine (Zhou and Neher 1993; Neher 1995) as well as calcium-binding proteins, such as calmodulin and S-100 (Feher et al. 1989; Hilt and Kligman 1991). In neuroendocrine cells and central synapses, the mobile calcium buffers appear to be parvalbumin, calretinin, and calbindin-28 kDa (Stuenkel 1994; Gabso et al. 1997; Muller et al. 2005, 2007; Schmidt et al. 2003). The role of particular intracellular buffers with various properties in the regulation of neurosecretion remains mostly undetermined, primarily in the neuromuscular synapses of rodents.

This modeling investigation, based on an analysis of diffusion and secretion kinetics, has shown that, in the absence of any Ca^{2+} buffers, the dynamics of calcium ion distribution in the active zone was identical in form at two values of Ca^{2+} flux that differed in size by a factor of three and thus accurately imitates experimental changes in the extracellular concentration of Ca^{2+} . Despite this, at an increased Ca^{2+} flux, the early phase of the TCS grew more rapidly at the expense of a higher number of transmitter quanta released with a shorter synaptic delay; that is, this early phase was accelerated in the model situation, when no buffers are assumed. Still, in the experimental work performed by ourselves (Samigullin et al. 2005; Bukharaeva et al. 2007) as well as by other authors (Barrett and Stevens 1972; Van der Kloot 1988; Parnas et al. 1986), no changes in the kinetics of the early phase of neurotransmitter secretion were found with a higher concentration of Ca^{2+} ,

and we can, therefore, assume that some retarding calcium buffers must be present in nerve terminals.

In addition, the absence of changes to the decay phase of the TCS during an increase in Ca^{2+} flux in the no-buffer model situation did not correspond to observed experimental data on the acceleration of the secretion process. This indicates the necessity of the additional participation of buffering systems in the regulation of the late phase of quanta release.

When a mobile buffer with a diffusion rate identical to the diffusion rate of free Ca^{2+} was used, we observed a decrease in the absolute value of the Ca^{2+} concentration maximum. This agrees with experimental data obtained from Purkinje cells, where it was shown that the mobile endogenous buffer calbindin decreased the amplitude of spatially distributed Ca^{2+} concentration (Schmidt et al. 2003). In experiments at neuromuscular junctions, we also observed a decrease in quantal content in the presence of a calcium buffer—BAPTA-AM (Bukharaeva et al. 2007), which indicates a lowering of intracellular calcium concentration.

The dynamics of changes in Ca^{2+} distribution in our simulation fits with observed changes in Ca^{2+} dynamics in cerebellar interneurons and in chromaffin cells in the presence of parvalbumin, another mobile endogenous buffer (Lee et al. 2000; Collin et al. 2005).

An analysis of the changes in secretion kinetics with regard to the role of a mobile buffer has shown that the TCS at two different values of Ca^{2+} flux were completely identical. Consequently, the acceleration of Ca^{2+} diffusion by a mobile buffer brought about the disappearance of differences in the kinetics of the early phase of secretion as were observed in the absence of the mobile buffer in the model system at different values of Ca^{2+} influx. On the other hand, the presence of a fixed buffer in the model with a diffusion coefficient equal to zero caused a retardation of the decrease in Ca^{2+} concentration at low values of Ca^{2+} flux compared to higher ones. We observed more prolonged phases of rise time and decay in the TCS at the lower value of Ca^{2+} flux. Such changes in the kinetics of Ca^{2+} concentration and the TCS can be explained by assuming that the fixed buffer obstructs Ca^{2+} diffusion.

After the influx is terminated, the Ca^{2+} -saturated fixed buffer acts as a slow source of free Ca^{2+} that leads to a retarded decay of calcium concentration in the secretion zone. This retardation is more pronounced at a low level of calcium flux and consequently leads to a higher desynchronization of the secretion process.

The results of mathematical modeling investigations in the presence of endogenous fixed and mobile calcium buffers fit with the changes in TCS that we observed in experiments at the neuromuscular junction of mice by varying the extracellular Ca^{2+} content and applying

exogenous buffers with rapid kinetics, such as BAPTA-AM (Samigullin et al. 2005; Bukharaeva et al. 2007). During the recording of uni-quantal endplate currents under increased concentrations of Mg^{2+} , it was found that a decrease in Ca^{2+} concentration from 0.4 to 0.2 mM produces, together with a decrease in quantal content, an increase in the fluctuation of synaptic delays, i.e., a desynchronization [Fig. 8(a,b)]. This was shown in the change of the cumulative curves constructed on the basis of synaptic delay histograms at high (0.4 mM) and low (0.2 mM) concentrations of Ca^{2+} [Fig. 8(c)].

Our mathematical modeling showed that the experimentally observed changes in the TCS, represented as cumulative curves of the histogram of released quanta, qualitatively occur when the nerve terminal contains a fixed nondiffusible calcium buffer, i.e., a buffer with molecules which change their position very little over the course of secretion compared with the distance between the calcium entry point and the secretion zone. Under these conditions, the changes in the model cumulative curves at high and low Ca^{2+} concentration are qualitatively identical with those experimentally observed [Fig. 9(a,b)]. The fixed buffer hinders calcium diffusion and keeps it in the active zone, which prolongs the stimulation of the active secretion zone and increases the asynchrony of neurotransmitter release. Quantitative differences between modeling and experimental data may exist because the living system differs even from a very comprehensive model. However, the qualitative agreement of the model and experiments demonstrates the important role of fixed and mobile calcium buffers in the regulation of quantal release kinetics.

It was shown in earlier experiments that the addition of an endogenous mobile calcium buffer under conditions of high desynchronization of secretion leads to a decrease in the degree of fluctuation of synaptic delays [Fig. 9(c)]; that is, it synchronized the release (Bukharaeva et al. 2007). Under the conditions of the model system described here, it was also observed that, in the presence of a fixed buffer, the addition of a mobile calcium buffer leads to changes in the time–space distribution of Ca^{2+} near the secretion zone because of the accelerated dispersion of the locally increased calcium concentration, which caused a synchronization of the neurosecretion process [Fig. 9(d)]. In chromaffin cells and cerebellar interneurons, the mobile buffer parvalbumin insignificantly decreased the peak amplitude of calcium concentration but speeded up its decay in the active zone (Lee et al. 2000; Collin et al. 2005); this is in good agreement with the results of our modeling.

Experimental and modeling studies (Soucek 1971; Giniatullin et al. 1995; Bukharaeva et al. 2002) demonstrated that alterations in the TCS or the degree of synchrony of quantal releases can modulate the amplitude of the integral endplate current. To assess the impact of these

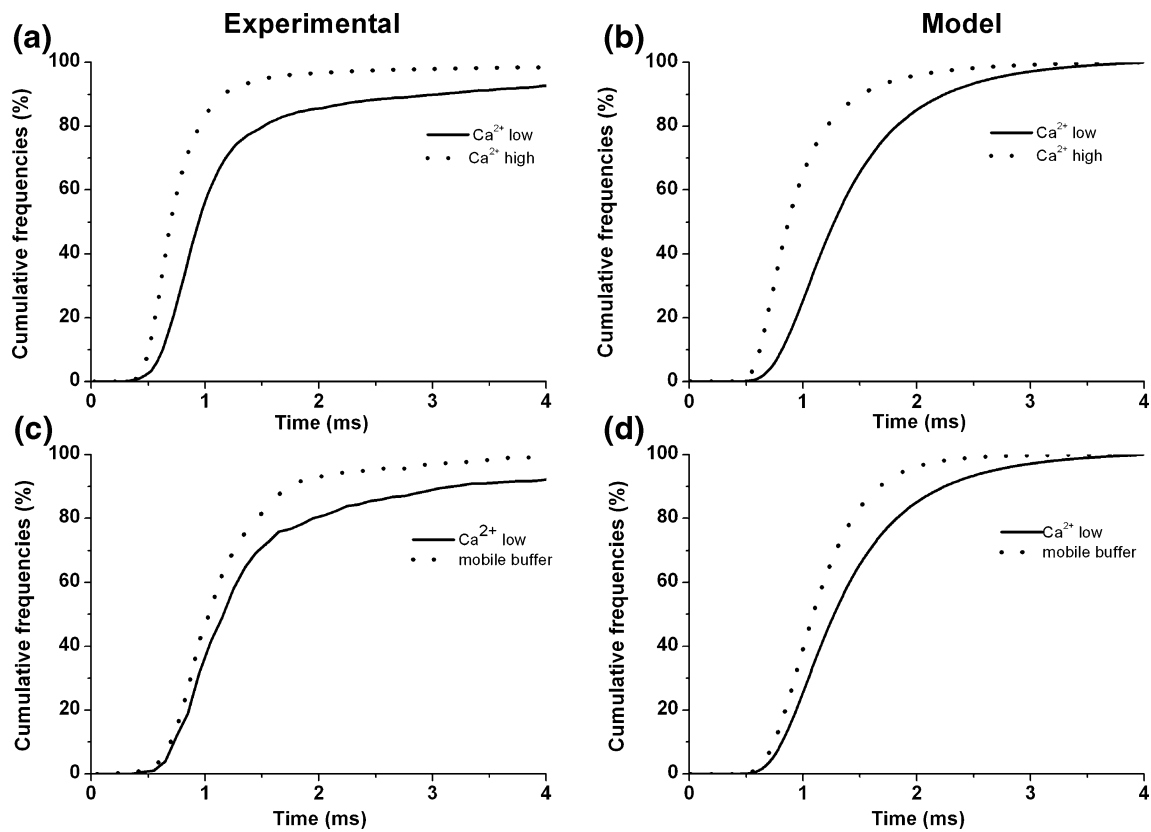


Fig. 9 (a) Experimental cumulative curves constructed from TCS with a low or high Ca^{2+} concentration. (b) Model cumulative curves constructed from TCS in Fig. 6(c) for various Ca currents. (c) Experimental cumulative curves constructed from synaptic latencies in

the control and in the presence of BAPTA-AM. (d) Model cumulative curves constructed from TCS in Fig. 7(c) with a low concentration of calcium and in the presence of a mobile buffer. The fixed buffer is taken into account in the modeling data

changes on the postsynaptic response peak amplitude, we constructed the multiquantal postsynaptic current by summation of the unquantal currents, the same as experimentally recorded miniature end-plate currents and, accordingly, their TCS with a fixed buffer and two different Ca^{2+} fluxes

[Fig. 10(a)] and their TCS with and without a mobile buffer with a low calcium content [Fig. 10(b)]. Note that the quantal content for all currents on Fig. 10 is the same. The constructed multiquantal response in the presence of a mobile buffer had a larger amplitude and shorter decay in

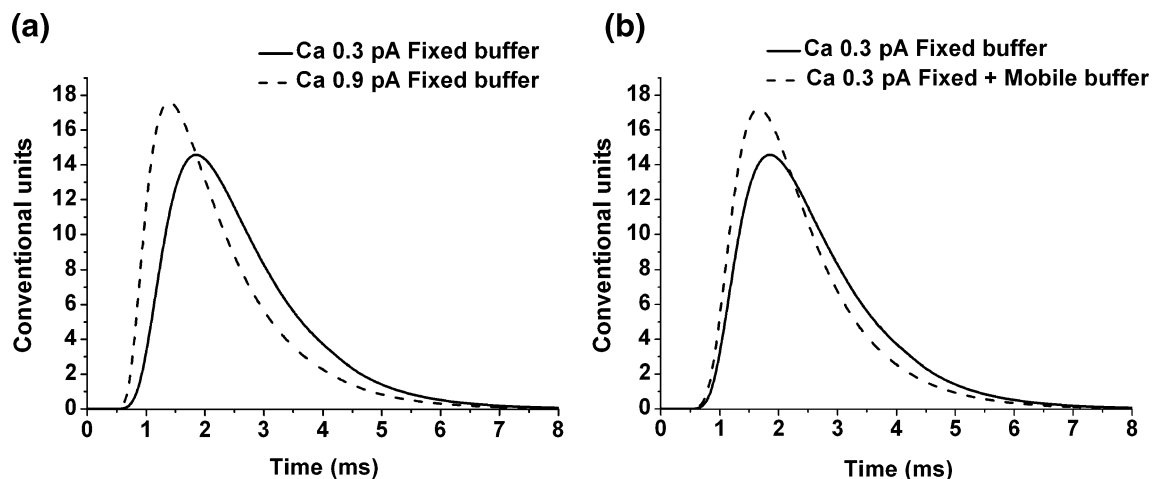


Fig. 10 Reconstruction of multiquantal postsynaptic responses according to the TCS with differing Ca^{2+} influx and with mobile and fixed buffers. Multiquantal responses were constructed from the experimentally measured parameters of unquantal end-plate currents according to TCS curves normalized to area by a convolution method.

The quantal content was equal in all cases. (a) Reconstructed responses for Ca currents of 0.3 and 0.9 pA according to TCS with fixed buffer [see Fig. 6(c)]. (b) Reconstructed responses for Ca current of 0.3 according to TCS with fixed buffer and with fixed and mobile buffer together [see Fig. 7(c)]

comparison with the response with only a fixed buffer [Fig. 10(b)] due to the faster decay of the TCS with a mobile buffer [Fig. 7(c)]. The increase in signal amplitude observed with fixed and mobile buffers also suggests that the synchronizing effect of buffers on release can have a strong impact on the amplitude of the multiquantal signals, even without a change in the number of quanta.

When quanta are released asynchronously, the amplitude of an integral postsynaptic response is smaller than during synchronous release. Therefore, when the release events are not sufficiently synchronized, the postsynaptic response may not reach the depolarization level critical for initiation of the postsynaptic action potential. Thus, the time course of quantal secretion is an important factor that determines the reliability of synaptic transmission.

Consistently, recent studies have demonstrated that the time course of quantal release is highly regulated and reflects the plasticity of the vesicular secretion (Sabatini and Regehr 1999; Lin and Farber 2002; Allana and Lin 2004). Thus, to understand how the reliability and strength of synaptic transmission can be regulated, we need to investigate how Ca^{2+} mediates the relative timings of quantal events (Naoki et al. 2005). The synchronism of the quantal release may not only play an important role in the neuromuscular junction, but may be crucial to the central synapses, where only a few quanta are released (Bi and Poo 1998), and in the processes of interaction between pre- and postsynaptic responses (Markram et al. 1997).

Acknowledgments We thank Dr. Maria Bykhovskaia and Dr. Andrey Skorinkin for critical reading of the manuscript. Supported by GAAVA5011411, GACR305/02/1333, and MSMT11310003 for FV, by RFBR 08-04-00923, Russian Scientific Schools—4177.2008.4 for EN, by “Russian Science Support Foundation” for DS, by US Civilian Research and Development Foundation (RUB1-2823-KA06) for EB and DS.

References

- Ahmed, Z., & Connor, J. (1988). Calcium regulation by and buffer capacity of molluscan neurons during calcium transients. *Cell Calcium*, *9*, 57–69.
- Allana, T., & Lin, J.-W. (2004). Relative distribution of Ca^{2+} channels at the crayfish inhibitory neuromuscular junction. *Journal of Neurophysiology*, *92*, 1491–5000.
- Augustine, G. J. (2001). How does calcium trigger neurotransmitter release? *Current Opinion in Neurobiology*, *11*, 320–326.
- Augustine, G. J., & Neher, E. (1992a). Calcium requirements for secretion in bovine chromaffin cells. *Journal of Physiology*, *450*, 247–271.
- Augustine, G. J., & Neher, E. (1992b) Neuronal Ca^{2+} signaling takes the local route. *Current Opinion in Neurobiology*, *2*, 302–307.
- Barrett, E. F., & Stevens, C. F. (1972). The kinetics of transmitter release at the frog neuromuscular junction. *Journal of Physiology*, *227*, 691–708.
- Bennett, M. R., Farnell, L., & Gibson, W. G. (2000). The probability of quantal secretion near a single calcium channel of an active zone. *Biophysical Journal*, *78*, 2201–2221.
- Bi, G., & Poo, M. (1998). Synaptic modifications in cultured hippocampal neurons: Dependence on spike timing, synaptic strength, and postsynaptic cell type. *Journal of Neuroscience*, *18*, 10464–10472.
- Bukharaeva, E., Samigullin, D., Nikolsky, E., & Magazanik, L. (2007). Modulation of the kinetics of evoked quantal release at mouse neuromuscular junctions by calcium and strontium. *Journal of Neurochemistry*, *100*, 939–949.
- Bukharaeva, E., Samigullin, D., Nikolsky, E., & Vyskočil, F. (2002). Protein kinase A cascade regulates quantal release dispersion at frog muscle endplate. *Journal of Physiology*, *538*, 837–848.
- Burnashev, N., & Rozov, A. (2005). Presynaptic Ca^{2+} dynamics, Ca^{2+} buffers and synaptic efficacy. *Cell Calcium*, *37*, 489–495.
- Chow, R., Klingauf, J., & Neher, E. (1994). Time course of Ca^{2+} concentration triggering exocytosis in neuroendocrine cells. *Proceedings of the National Academy of Sciences of the United States of America*, *91*, 12765–12769.
- Collin, T., Chat, M., Lucas, M., Moreno, H., Racay, P., Schwaller, B., et al. (2005). Developmental changes in parvalbumin regulate presynaptic Ca^{2+} signaling. *Journal of Neuroscience*, *25*, 96–107.
- Dodge, J., & Rahamimoff, R. (1967). Co-operative action a Ca^{2+} in transmitter release at the neuromuscular junction. *Journal of Physiology*, *193*, 419–432.
- Glavinovich, M., & Rabie, H. (2001). Monte Carlo evaluation of quantal analysis in the light of Ca^{2+} dynamics and the geometry of secretion. *Pflügers Archiv—European Journal of Physiology*, *443*, 132–145.
- Feher, J., Fulmer, C., & Fritzsche, G. (1989). Comparison of the enhanced steady-state diffusion of calcium by calbindin-D9K and calmodulin, possible importance in intestinal calcium absorption. *Cell Calcium*, *10*, 189–203.
- Gabso, M., Neher, E., & Spira, M. (1997). Low mobility of the Ca^{2+} buffers in axons of cultured Aplysia neurons. *Neuron*, *18*, 473–481.
- Giniatullin, R., Kheeroug, L., & Vyskočil, F. (1995). Modelling endplate current: Dependence on quantum secretion probability and postsynaptic miniature current parameters. *European Journal of Biophysics*, *23*, 443–446.
- Hilt, D., & Kligman, D. (1991). *The S-100 protein family, a biochemical and functional overview. Novel calcium-binding proteins* (pp. 65–103). Berlin: Springer.
- Katz, B. (1968). The role of calcium in neuromuscular facilitation. *Journal of Physiology*, *195*, 481–492.
- Katz, B., & Miledi, R. (1965). The measurement of synaptic delay, and the time course of acetylcholine release at the neuromuscular junction. *Proceedings of the Royal Society of London. Series B, Biological Sciences*, *161*, 483–495.
- Kits, K., de Vlieger, T., Kooi, B., & Mansvelder, H. (1999). Diffusion barriers limit the effect of mobile calcium buffers on exocytosis of large dense cored vesicles. *Biophysical Journal*, *76*, 1693–1705.
- Klingauf, J., & Neher, E. (1997). Modeling buffered Ca^{2+} diffusion near the membrane, implications for secretion in neuroendocrine cells. *Biophysical Journal*, *72*, 674–690.
- Lee, S., Schwaller, B., & Neher, E. (2000). Kinetics of Ca^{2+} binding to parvalbumin in bovine chromaffin cells, implications for $[\text{Ca}^{2+}]$ transients of neuronal dendrites. *Journal of Physiology*, *525*, 419–432.
- Lin, J. W., & Farber, S. (2002). Modulation of synaptic delay during synaptic plasticity. *Trends in Neuroscience*, *25*, 449–455.
- Lin, J. W., Fu, Q., & Allana, T. (2005). Probing the endogenous Ca^{2+} buffers at the presynaptic terminals of the crayfish neuromuscular junction. *Journal of Neurophysiology*, *94*, 377–386.

- Markram, H., Lubke, J., Frotscher, M., & Sakmann, B. (1997). Regulation of synaptic efficacy by coincidence of postsynaptic APs and EPSPs. *Science*, *275*, 213–216.
- Matveev, V., Sherman, A., & Zucker, R. (2002). New and corrected simulations of synaptic facilitation. *Biophysical Journal*, *83*, 1368–1373.
- Matveev, V., Zucker, R., & Sherman, A. (2004). Facilitation through buffer saturation, constraints on endogenous buffering properties. *Biophysical Journal*, *86*, 2691–2709.
- Meinrenken, C., Borst, J., & Sakmann, B. (2002). Calcium secretion coupling at Calyx of Held governed by nonuniform channel-vesicle topography. *Journal of Neuroscience*, *22*, 1648–1667.
- Muller, A., Kukley, M., Stausberg, P., Beck, H., Muller, W., & Dietrich, D. (2005). Endogenous Ca^{2+} buffer concentration and Ca^{2+} microdomains in hippocampal neurons. *Journal of Neuroscience*, *25*, 558–565.
- Muller, M., Felmy, F., Schwaller, B., & Schneggenburger, R. (2007). Parvalbumin is a mobile presynaptic Ca^{2+} buffer in the Calyx of Held that accelerates the decay of Ca^{2+} and short-term facilitation. *Journal of Neuroscience*, *27*, 2261–2271.
- Nauki, H., Sakumura, Y., & Ishii, S. (2005). Local signaling with molecular diffusion as a decoder of Ca^{2+} signals in synaptic plasticity. *Molecular Systems Biology*, *1*, 0027.
- Neher, E. (1995). The use of fura-2 for estimating Ca buffers and Ca fluxes. *Neuropharmacology*, *34*, 1423–1442.
- Nowycky, M., & Pinter, M. (1993). Time courses of calcium and calcium-bound buffers following calcium influx in a model cell. *Biophysical Journal*, *64*, 77–91.
- Parnas, H., Dudel, J., & Parnas, I. (1986). Neurotransmitter release and its facilitation in crayfish. V. Another voltage-dependent process beside Ca entry controls the time course of phasic release. *Pflügers Archiv*, *406*, 121–130.
- Sabatini, B., & Regehr, W. (1999). Timing of synaptic transmission. *Annual Review Physiology*, *61*, 521–42.
- Sala, F., & Hernandez-Cruz, A. (1990). Calcium diffusion modeling in a spherical neuron. Relevance of buffering properties. *Biophysical Journal*, *57*, 313–324.
- Samigullin, D., Bukharaeva, E., Vyskočil, F., & Nikolsky, E. (2005). Calcium dependence of uni-quantal release latencies and quantal content at mouse neuromuscular junction. *Physiological Research*, *54*, 129–132.
- Schmidt, H., Stiefel, K., Racay, P., Schwaller, B., & Eilers, J. (2003). Mutational analysis of dendritic Ca^{2+} kinetics in rodent Purkinje cells, role of parvalbumin and calbindin D28k. *Journal of Physiology*, *551*, 13–32.
- Schneggenburger, R., & Neher, E. (2000). Intracellular calcium dependence of transmitter release rates at a fast central synapse. *Nature*, *406*, 889–893.
- Schneggenburger, R., & Neher, E. (2005). Presynaptic calcium and control of vesicle fusion. *Current Opinion in Neurobiology*, *15*, 266–274.
- Segura, J., Gil, A., & Soria, B. (2000). Modeling study of exocytosis in neuroendocrine cells, influence of the geometrical parameters. *Biophysical Journal*, *79*, 1771–1786.
- Shahrezaei, V., & Delaney, K. R. (2004). Consequences of molecular-level Ca^{2+} channel and synaptic vesicle colocalization for the Ca^{2+} microdomain and neurotransmitter exocytosis: A Monte Carlo study. *Biophysical Journal*, *87*, 2352–2364.
- Shahrezaei, V., Cao, A., & Delaney, K. (2006). Ca^{2+} from one or two channels controls fusion of a single vesicle at the frog neuromuscular junction. *Journal of Neuroscience*, *26*, 13240–13249.
- Soucek, B. (1971). Influence of latency fluctuations and the quantal process of transmitter release on the end-plate potential's amplitude distribution. *Biophysical Journal*, *11*, 127–139.
- Stockbridge, N., & Moore, J. (1984). Dynamics of intracellular calcium and its possible relationship to phasic transmitter release and facilitation at the frog neuromuscular junction. *Journal of Neuroscience*, *4*, 803–811.
- Stuenkel, E. (1994). Regulation of intracellular calcium and calcium buffering properties of rat isolated neurohypophysial nerve endings. *Journal of Physiology*, *481*, 251–271.
- Tang, Y., Schlumpberger, T., Kim, T., Lueker, M., & Zucker, R. (2000). Effects of mobile buffers on facilitation, experimental and computational studies. *Biophysical Journal*, *78*, 2735–2751.
- Van der Kloot, W. (1988). The kinetics of quantal releases during end-plate currents at the frog neuromuscular junction. *Journal of Physiology*, *402*, 605–626.
- Yamada, W., & Zucker, R. (1992). Time course of transmitter release calculated from simulations of a calcium diffusion model. *Biophysical Journal*, *61*, 671–682.
- Zhou, Z., & Neher, E. (1993). Mobile and immobile calcium buffers in bovine adrenal chromaffine cells. *Journal of Physiology*, *469*, 245–273.